

Submitted as: “Tools in Protein Science” article

An *in vitro* mimic of in-cell solvation for protein folding studies

Caitlin M. Davis^{1,2,*†}, Jonathan Deutsch³, and Martin Gruebele^{1,2,3,*}

¹*Department of Physics*, ²*Department of Chemistry*, and ³*Center for Biophysics and Quantitative Biology*, University of Illinois at Urbana-Champaign, Urbana, IL 61801 USA

***Corresponding authors:**

Email: c.davis@yale.edu, mgruebel@illinois.edu

†Current address:

Department of Chemistry, Yale University, 255 Prospect Street, New Haven, CT 06520

Running Title: *In vitro* mimic for in-cell folding

Total number of manuscript pages: 21

Total number of supplementary material pages: 5

Number of tables: 0

Number of Figures: 4

Supplementary Material:

Supplementary material includes plots of thermal stability as a function of crowding agent, the complete set of *in vitro* equilibrium temperature denaturation measurements, representative melt curves collected in living U-2 OS cells, and complete tables of thermodynamic and kinetic parameters obtained *in vitro* and in living U-2 OS cells. See SupplementToInVitroMimic.pdf

Abstract

Ficoll, an inert macromolecule, is a common *in vitro* crowder, but by itself it does not reproduce in-cell stability or kinetic trends for protein folding. Lysis buffer, which contains ions, glycerol as a simple kosmotrope, and mimics small crowders with hydrophilic/hydrophobic patches, can reproduce sticking trends observed in cells, but not the crowding. We previously suggested that the proper combination of Ficoll and lysis buffer could reproduce the opposite in-cell folding stability trend of two proteins: VlsE is destabilized in eukaryotic cells and PGK is stabilized. Here, to discover a well-characterized solvation environment that mimics in-cell stabilities for these two very differently-behaved proteins, we conduct a two-dimensional scan of Ficoll (0-250 mg/ml) and lysis buffer (0-75%) mixtures. Contrary to our previous expectation, we show that mixtures of Ficoll and lysis buffer have a significant nonadditive effect on the folding stability. Lysis buffer enhances the stabilizing effect of Ficoll on PGK and inhibits the stabilizing effect of Ficoll on VlsE. We demonstrate that a combination of 150 mg/ml Ficoll and 60% lysis buffer can be used as an *in vitro* mimic to account for both crowding and non-steric effects on PGK and VlsE stability and folding kinetics in the cell. Our results also suggest that this mixture is close to the point where phase separation will occur. The simple mixture proposed here, based on commercially available reagents, could be a useful tool to study a variety of cytoplasmic protein interactions, such as folding, binding and assembly, and enzymatic reactions.

Keywords (4-10 words)

fluorescence resonance energy transfer (FRET), laser-induced temperature jump, macromolecular crowding, phosphoglycerate kinase (PGK), protein folding, quinary interactions, thermal denaturation, variable major protein-like sequence expressed (VlsE)

Statement

The complexity of the in-cell environment is difficult to reproduce in the test tube. Here we validate a mimic of cellular crowding and sticking interactions in a test tube using two proteins that are differently impacted by the cell: one is stabilized and the other is destabilized. This mimic is a starting point to reproduce cellular effects on a variety of protein and biomolecular interactions, such as folding and binding.

Introduction

Protein stability and kinetics are typically studied in dilute aqueous buffer. Buffer components are selected for their solubility in water, chemical stability, ability to buffer at the desired pH, compatibility with other buffer components, and planned experiments. For example, phosphate buffers are often selected for temperature-dependent studies at physiological pH because their pK_a is relatively insensitive to temperature and phosphate is a common anion in the cell. Yet these experiments are limited in their ability to reproduce measurements made inside cells.¹

Discrepancies between *in vitro* and in-cell measurements often arise because traditional buffers do not account for the local environment of proteins inside cells. The interior of the cell is crowded and heterogenous, with 30-40% of its volume comprised of ions, small metabolites, and macromolecules.² Since two macromolecules cannot occupy the same space in solution, crowding results in steric hinderance or repulsion, limiting the volume available to other solutes. The thermodynamic consequences of macromolecular crowding are described by the excluded volume effect.³ To mimic cellular crowding *in vitro*, inert macromolecules such as dextran, Ficoll, polyethylene glycol (PEG) or proteins (e.g. albumin) can be added to the buffer.⁴ *In vitro* studies with inert macromolecules added to the buffer demonstrate that crowding compacts and stabilizes proteins,^{5,6} modulates enzymatic activity,^{7,8} and enhances association.⁹ Yet crowding alone cannot account for all interactions inside cells; Superoxide dismutase (SOD1),¹⁰ variable major protein-like sequence expressed (VlsE),^{11,12} B1 domain of protein G (GB1),¹³ and chymotrypsin inhibitor 2 (CI2)¹⁴ all are destabilized inside cells compared to *in vitro*.

Inert crowders alone neglect that macromolecules may be attracted by or repelled from each other inside cells. Non-steric interactions refer to all interactions between the protein and its environment aside from volume-excluding steric interactions, encompassing non-specific sticking between macromolecules and weak quinary interactions evolved for function.¹⁵ The surface of proteins is particularly important in determining the strength of non-steric interactions, which can be stabilize or destabilize proteins¹⁶⁻¹⁹ and suppress or activate enzymes²⁰. To mimic non-steric interactions *in vitro*, dilute cell lysate or lysis buffer can be added to the buffer.^{6,16-18} However, neither simple extrapolation of measurements in a non-steric mimic nor steric mimic at in-cell concentrations near 300 mg/ml have been able to reproduce in-cell observations by themselves.⁶

We previously speculated that a buffer combining Ficoll (steric agent) and lysis buffer (ion/small molecule agent) could be useful as an *in vitro* mimic that accounts for both crowding and non-specific interactions in the cell.⁶ Here we test how the ratio of Ficoll and lysis buffer

affects folding of phosphoglycerate kinase (PGK, stabilized inside cells) and a bacterial surface protein (VlsE, destabilized inside cells).²¹ We compare the stability and folding rates of PGK and VlsE in a range of Ficoll and lysis buffer mixtures with measurements in living U-2 OS cells. We find that the effects of lysis buffer and Ficoll are not simply additive. Lysis buffer enhances the stabilizing effect of Ficoll on PGK and inhibits the stabilizing effect of Ficoll on VlsE. We identify a mixture that reproduces the in-cell stability and kinetics of both proteins: 150 mg/ml Ficoll and 60% lysis buffer. We propose that this combination could be useful as an *in vitro* mimic of crowding and non-specific interactions in cells for cytoplasmic protein interactions such as folding, binding and assembly, and enzymatic reactions. We also find that this combination is close to, but not at the point where phase separation occurs, and suggest a hypothesis of why this may also be representative of the in-cell environment.

Results and Discussion

PGK and VlsE FRET constructs and denaturation measurements

Yeast PGK [Fig. 1(A)] and *Borrelia burgdorferi* VlsE [Fig. 1(B)] were selected as model proteins for these studies because they have opposite stability trends when moved from *in vitro* into cells. In sodium phosphate buffer PGK and VlsE have similar melting temperatures, $T_m = 39 \pm 1$ °C and $T_m = 40 \pm 1$ °C, respectively.^{6,12,22} However, inside U-2 OS cells PGK is stabilized, $T_m = 44 \pm 2$ °C,^{21,22} and VlsE is destabilized, $T_m = 35 \pm 2$ °C.¹¹ The proteins were FRET-labeled to enable direct comparison between *in vitro* and in-cell measurements. A green fluorescent protein (AcGFP1) donor (D) was cloned to the N-terminus and a mCherry acceptor (A) was cloned to the C-terminus of the protein. Thermal denaturation was monitored using the donor fluorescence-acceptor fluorescence ratio (D/A), which reports on the end-to-end distance of the FRET construct. A large D/A occurs when there is less FRET, such as in the unfolded state, while a low D/A corresponds to high FRET such as a folded state. For simplicity we refer to the FRET-labeled constructs as PGK and VlsE.

Mimics of crowding and sticking

To identify conditions that produce the correct balance of steric and non-steric interactions to reproduce in-cell observations, PGK and VlsE stability was measured in combinations of Ficoll PM 70 and Pierce IP lysis buffer, as suggested in our previous work on cell lysate/Ficoll.⁶ Ficoll

PM 70 is a relatively inert, 70kD highly-branched copolymer of sucrose and epichlorohydrin building blocks, and a common choice for steric crowding agent.²³ Comparison of the effect of common steric crowding agents, PEG and Ficoll, between 0.3 and 70 kD on PGK stability shows that they follow similar trends, with larger crowders having a greater stabilizing effect on PGK than smaller crowders (Fig. S1). Crowders larger than Ficoll PM 70 were not tested because of their reduced solubility. In principle the reported study could be reproduced with smaller crowding agents, but we anticipate that this would require higher concentrations of crowders to achieve the same result.

Considerations for lysis buffer selection should include the host organism, protein localization, and ability to maintain protein complexes. Pierce IP lysis buffer was selected because it is a commercially available moderate-strength lysis buffer for mammalian whole cell lysis and is optimized to minimize disruption of protein complexes for pull-down and immunoprecipitation assays. Pierce IP lysis buffer, which we recently showed reproduces the sticking trends observed in dilute cell lysate,⁶ contains ions (150 mM NaCl), small organics (25 mM tris, 1 mM EDTA), kosmotropes (5% glycerol), and a mimic of short chain fatty acids and/or small crowders with hydrophilic and hydrophobic patches (1% NP-40). We refer to these from now on as “Ficoll” and “lysis buffer” for simplicity.

We found that high physiological concentrations of Ficoll, 300-400 mg/ml,² are insoluble in 100% lysis buffer and induce protein aggregation. Therefore, the crowding effect of Ficoll was tested to a maximum concentration of 250 mg/ml in 50 mg/ml increments and the sticking effect of lysis buffer was tested to 75% v/v in $\approx 20\%$ v/v increments, conditions that maintained buffer solubility and protein stability (see Materials and Methods). In the context of in-cell phase separation, e.g. reversible membraneless organelles,²⁴ it is interesting to note that Ficoll/lysis buffer conditions that mimic the in-cell environment best (see below) are not far from conditions where proteins stick and aggregate. In order to foster interactions such as protein-protein signaling or storage in liquid droplets, the cell environment must promote interactions, but not too much.

The effects of Ficoll and lysis buffer on stability are non-additive

The melting curves of PGK and VlsE [Fig. S2] in mixtures of Ficoll and lysis buffer were fit to an apparent two-state equilibrium model [Equation 1]. Consistent with past *in vitro* measurements, the melting temperatures in sodium phosphate buffer are $T_m = 38 \pm 1$ °C for PGK and $T_m = 40 \pm 1$ °C

for VlsE. In order to highlight the different effects of crowding and solvent composition, we display the same dataset in two ways. First, the melting temperatures at constant lysis buffer concentration (0-75% v/v) are reported as a function of Ficoll (0-250 mg/ml) in Fig. 2A-2B. Second, the melting temperatures at constant Ficoll concentration (0-250 mg/ml) are reported as a function of lysis buffer (0-75% v/v) in Fig. 2C-2D. Thermodynamic parameters derived from two-state fits of the melting curves are reported in Table S1-S4.

Independently, lysis buffer and Ficoll have qualitatively similar effects on PGK and VlsE. Without Ficoll, both proteins are destabilized by ≈ 5 °C at the maximum lysis buffer concentration tested [Fig. 2C-2D]. Without lysis buffer, VlsE and PGK are only slightly stabilized (≤ 2 °C) at the maximum Ficoll concentration tested [Fig. 2A-2B].

There are two significant differences between the behaviors of PGK and VlsE that suggest that VlsE is more sensitive to non-steric interactions (“sticking”) than PGK. First, VlsE is more rapidly destabilized than PGK by low lysis buffer concentration (20%). Second, VlsE is actually destabilized by the lowest Ficoll concentration (50 mg/ml), before addition of more Ficoll increases its stability. At the lowest tested Ficoll concentration, 50 mg/ml, even a relatively inert crowder like Ficoll provides more sticking than crowding, resulting in destabilization of VlsE. Similarly, low and high concentrations of simple macromolecular crowding agents have been shown to have opposite effects on binding affinity.^{25,26} These observations are consistent with our past studies of PGK and VlsE in Ficoll and cell lysate, which showed that PGK and VlsE are stabilized by high concentrations of Ficoll and that VlsE is more sensitive to non-steric interactions than PGK.⁶

The effects of lysis buffer and Ficoll in Fig. 2 are not additive. Assuming for a moment that these effects are additive compared to sodium phosphate buffer as a reference (0% lysis buffer, 0 mg/ml Ficoll), PGK is destabilized by ≈ 5 °C in 75% lysis buffer and stabilized by ≈ 2 °C in 250 mg/ml Ficoll [Fig. 2A, 2C], so we expect PGK to have a net destabilization of ≈ 3 °C in a mixture of 75% lysis buffer and 250 mg/ml Ficoll. However, PGK is not destabilized at all in a mixture of 75% lysis buffer and 250 mg/ml Ficoll, rather it is stabilized by ≈ 8 °C compared to sodium phosphate buffer [Fig. 2A, 2C]. The same logic can be used to demonstrate that the effects of lysis buffer and Ficoll on the stability of VlsE are not additive either [Fig. 2B, 2D].

Instead, we observe that lysis buffer enhances the stabilizing effect of Ficoll on PGK and inhibits the stabilizing effect of Ficoll on VlsE [Fig. 2A-2B]. We assess the relative stability by

comparing the slope, $\Delta\text{Stability } (^{\circ}\text{C})/\Delta\text{Ficoll (mg/ml)}$, at a given lysis buffer condition. For PGK, the minimum slope is observed at 0% lysis buffer and the maximum slope is observed at 75% lysis buffer [Fig. 2A]. Therefore, lysis buffer enhances the stabilizing effect of Ficoll on PGK. Conversely, lysis buffer suppresses the stabilizing effect of Ficoll on VlsE. For VlsE, the minimum slope is observed at 75% lysis buffer and the maximum slope is observed at 0% and 20% lysis buffer [Fig. 2B]. The non-additive effect offers the possibility that a special Ficoll/lysis buffer combination could mimic the opposite trends observed in-cell for these two proteins.

60% lysis buffer and 150 mg/ml Ficoll reproduce in-cell stability of both PGK and VISE

To determine the specific mixture of lysis buffer and Ficoll that best mimics the effects of crowding and non-specific interactions inside cells on the stability of these two proteins, the difference between *in vitro* stability and in-cell melting temperature ($\Delta T_m = T_{m,\text{in vitro}} - T_{m,\text{in cell}}$) in each mixture of Ficoll and lysis buffer was calculated. A heat map of these differences (ΔT_m) is reported in Fig. 3, referenced to either phosphate buffer (top row) or in-cell data (bottom row). Red indicates *in vitro* conditions more stable than the reference, and blue indicates conditions that are less stable than the reference. (To make full use of the color range, in the top row zero difference relative to phosphate buffer is light pink, whereas in the bottom row zero difference relative to U-2 OS cells is light blue.) Representative in-cell melting curves of PGK and VlsE [Fig. S3] and thermodynamic parameters derived from two-state fits of the melting curves [Table S5-S6] are reported in the supporting information.

Protein stability landscapes are complex, with conditions that can mimic in-cell stability lying neither at a maxima or minima of the Ficoll or lysis buffer ranges we explored (Fig. 3). In fact, there are several mixtures of Ficoll and lysis buffer that can adequately reproduce in-cell stability separately for PGK or VlsE. For PGK (Fig. 3, left), there are two areas on the landscape that mimic the cell $\pm 1^{\circ}\text{C}$, both at Ficoll concentrations ≥ 150 mg/ml and separated by a trough at 40% lysis buffer. The in-cell stability of VlsE can be mimicked $\pm 1^{\circ}\text{C}$ across a wide range of conditions between 20-60% lysis buffer and 0-150 mg/ml Ficoll. Consistent with past observations,⁶ neither lysis buffer nor Ficoll alone are able to reproduce both the in-cell stabilization of PGK and the in-cell destabilization of VlsE.

The condition that best reproduces in-cell stability of both VlsE and PGK simultaneously is at 150 mg/ml Ficoll and 60% lysis buffer, outlined in black in Fig. 3. This condition is defined as the

minimum of the sum of the absolute value of the difference between in cell and *in vitro* melting temperature of PGK and VlsE [$\min(|\Delta T_{m, \text{PGK}}| + |\Delta T_{m, \text{VlsE}}|)$]. 150 mg/ml Ficoll is close to the 160 mg/ml Ficoll we recently predicted by linear interpolation,⁶ although we actually find significant non-additivity here. 150 mg/ml Ficoll is at the low end of physiologically relevant levels of macromolecular crowding.²⁷ This highlights the importance of considering macromolecular crowding together with non-specific interactions. Transient interactions between proteins and small organics or osmolytes modulate protein stability further inside cells.²⁸

The mimic buffer reproduces VlsE's, but not quite PGK's, in-cell folding relaxation rate

An ideal *in vitro* mimic of the in-cell solvation environment would not only reproduce protein stability but also folding relaxation rates. Stability and folding rates are not necessarily correlated. However, many proteins have a linear “chevron plot” across a broad range of solvent conditions,²⁹ demonstrating a correlation between stability and folding rate. For example, for proteins that fold via a two-state mechanism, the free energy of stability ΔG_u and relaxation rate $k_{obs} = k_f + k_u$ are not independent and can be related by $\Delta G_u = RT \ln(k_f/k_u)$. Our past studies of PGK and VlsE showed that there is a linear correlation between the stability and relaxation rate of VlsE in Ficoll or lysis buffer, but not for PGK.⁶ Therefore, we predict that our cellular mimic will accurately reproduce the kinetics of VlsE, but not necessarily PGK.

FReI was used to measure relaxation dynamics near $\Delta G_u = 0$ ($k_f \approx k_u$) following a temperature jump to the melting temperature in living U-2 OS cells and buffer (Fig. 4). The optimal buffer mimic of in-cell protein stability, sodium phosphate with 60% lysis buffer and 150 mg/ml Ficoll, is compared with three extremes, sodium phosphate buffer, sodium phosphate buffer with 250 mg/ml Ficoll, and sodium phosphate buffer with 75% lysis buffer. The transients are fit to a double exponential where the first exponential accounts for the instrument response and relaxation of AcGFP1 and the second exponential is the protein relaxation kinetics of interest [Equation 2]. Thermodynamic parameters derived from the fits are reported in Table S5-S7.

As anticipated, the cellular mimic reproduces the folding kinetics of VlsE more accurately than PGK's. Inside cells the relaxation times of VlsE and PGK we measured here are $\tau = 2.9 \pm 0.7$ s and $\tau = 3.0 \pm 0.9$ s, respectively. In sodium phosphate buffer the relaxation time of both proteins is faster, VlsE $\tau = 0.9 \pm 0.1$ s and PGK $\tau = 1.4 \pm 0.1$ s. VlsE is more sensitive to non-steric sticking interactions than crowding.⁶ Indeed, VlsE's folding is slowed to ≈ 2.5 s in mixtures including lysis buffer and

unaffected by the addition of Ficoll (Fig. 4). The folding of PGK is relatively insensitive to the *in vitro* solvation environment: addition of Ficoll, lysis buffer, or a mixture of Ficoll and lysis buffer does nothing to slow the dynamics of PGK (Fig. 4). Our in-cell mimic conditions of 60% lysis buffer and 150 mg/ml Ficoll slightly overestimate the observed in-cell relaxation rate.

Substitution of the 27 kD mCherry on PGK with a small ReAsH tag speeds the folding of PGK in cells by a factor of 2, nearly reproducing the *in vitro* folding relaxation rate.³⁰ Therefore, interactions between the tag and the cytoplasmic matrix are not fully captured by our Ficoll and lysis buffer mimics. Such interactions may slow down chain diffusion, resulting in the slower observed folding rates in cells.³¹

Conclusions

The right mixture of Ficoll and lysis buffer can be used to reproduce in-cell protein stability and kinetics. A protein stabilization landscape can be generated from a series of mixtures of Ficoll and lysis buffer. These landscapes are complex, with conditions that mimic in-cell stability lying neither at maxima or minima of the Ficoll and lysis buffer concentration ranges we tested. The effects of lysis buffer, a non-steric sticking agent, and Ficoll, a steric crowding agent, are protein-specific and non-additive. Lysis buffer enhances the stabilizing effect of Ficoll on PGK and inhibits the stabilizing effect of Ficoll on VlsE. We propose a mechanism analogous to the non-additive effect of charged guanidinium ions and neutral urea on protein unfolding: the combination of the two chaotropes actually leads to more compact unfolded states than either alone,³² with the proposed explanation that preferential binding of guanidinium/urea to charged/uncharged residues provides the best electrostatic screening and most compact unfolded state.^{32,33} In our case, VlsE is generally known to be more sensitive to sticking interactions. Thus, the components of lysis buffer may be more effective in binding to and denaturing VlsE and screening it from the stabilizing influence of Ficoll. In very general terms, the competition between specific binding and long-range screening effects on solvent non-additivity has been invoked in numerous cases, of which ours is just a specific example.^{32,33}

For PGK and VlsE, the mixture that best reproduces the in-cell stability and kinetics of both proteins simultaneously is 150 mg/ml Ficoll and 60% lysis buffer. We propose this combination as an *in vitro* mimic of crowding and non-specific interactions in cells. Already, we have observed that non-optimized mixtures of steric (Ficoll) and non-steric (cell lysate) mixtures are able to

suppress non-functional aggregation that is not observed in-cell, such as for the ATP-dependent association of heat shock function of Hsp70 with its non-obligatory client PGK.³⁴ From a practical standpoint, there are several advantages to using an *in vitro* mimic: (1) cell populations are heterogeneous, (2) buffers are easily reproduced and (3) more biophysical characterization methods are available *in vitro*. We demonstrated this approach works for two extreme cases of protein stability in cells, and therefore we expect that this could be a useful approach to study other cytoplasmic protein interactions, for example folding, binding and assembly, and enzymatic reactions.

Materials and Methods

Protein Engineering and Expression So that temperature-dependent experiments could be conducted inside U-2 OS cells at near-physiological temperatures, we used previously described FRET-labeled variants of VlsE¹¹ and PGK²¹ with melting temperatures around 40 °C. Briefly, we used an enzymatically active triple mutant (Y122W/W308F/W333F) of yeast PGK²¹ and a variant of bacterial VlsE¹¹ without the N-terminal lipidation signal. The FRET-labeled fusion proteins were constructed by ligating the genes for AcGFP1 and mCherry to the N and C termini, respectively. A two-amino acid linker was placed between the protein and label. Additionally, a His tag with a thrombin cleavage site was added to the N-terminus of PGK-FRET and C-terminus of VlsE-FRET for purification of the recombinant protein using a Ni affinity column. The fusion protein constructs were cloned into the pDream 2.1 expression plasmid (GenScript Biotech, Piscataway, NJ).

For *in vitro* studies, VlsE and PGK were expressed and purified as previously reported.⁶ The purified proteins were identified using SDS-page and dialyzed into sodium phosphate storage buffers pH 7 (10 mM for VlsE and 20 mM for PGK). The concentrations were calculated using Beer's law from the absorbance of AcGFP1 at 475 nm and its extinction coefficient of 32,500 L⁻¹ mol⁻¹ cm⁻¹. The molecular weight of PGK was confirmed using low-resolution electrospray ionization mass spectrometry. The protein's properties were further analyzed by their circular dichroism and fluorescence spectrums to confirm tertiary structure was not disrupted by labeling and/or purification. Sample concentrations of 3 μM were prepared for *in vitro* studies by

sandwiching the sample between a coverslip and microscope slide with a 100 μm spacer. The same imaging chambers were used for *in vitro* and in-cell studies.

Buffer Preparation *In vitro* measurements were conducted for a matrix of buffer conditions, consisting of a mixture of Ficoll PM 70 (Sigma-Aldrich, St. Louis, MO) between 0 and 250 mg/ml and Pierce IP lysis buffer (25 mM Tris-HCl pH 7.4, 150 mM NaCl, 1 mM EDTA, 1% NP-40 and 5% glycerol) between 0 and 75% v/v. Stock Ficoll solutions of ≈ 400 mg/ml were prepared by slowly stirring Ficoll into sodium phosphate buffer or Pierce IP lysis buffer under gentle heat. To ensure complete solubilization of Ficoll, the final concentration of Ficoll and Pierce IP lysis buffer was sonicated for 10 min immediately prior to the addition of protein and stability measurement.

Cell Culture and Transfection Human bone osteosarcoma epithelial cells (U-2 OS) were cultured and grown to 70% confluency in DMEM (Corning, Corning, NY) + 1% penicillin-streptomycin (Corning) + 10% fetal bovine serum (FBS, ThermoFisher Scientific) media. Transfection was performed with Lipofectamine (Invitrogen) following the manufacturer's protocol. At the time of transfection, cells were split and grown on coverslips. Media was changed six hours after transfection. Cells were imaged in OptiMEM media (ThermoFisher Scientific) supplemented with 10% FBS 17 hours after transfection.

Fast Relaxation Imaging (FReI) The FReI apparatus has been described previously.³⁵ Briefly, a computer-controlled, continuous-wave 2 μm laser (AdValue Photonics, Tucson, AZ) is used to rapidly apply a step-function shaped temperature perturbation to the sample. As long as the perturbation is applied at a time scale faster than the underlying conformational dynamics (T-jump), it will elicit a time-dependent response in the protein's FRET signal that can be used to probe the reaction. The stepped perturbation begins at ≈ 21 $^{\circ}\text{C}$ and increases to ≈ 50 $^{\circ}\text{C}$ in 4 $^{\circ}\text{C}$ steps. The protein is given ≈ 9 seconds to relax to its new equilibrium following each jump.

A microscope objective (Zeiss 63x/0.85 NA N-Achroplan) images the fluorescence from the laser-heated field of view onto a CMOS camera (Lumenera LT225 NIR/SCI CMOS detector), which collects snapshots of green and red fluorescence at a frame rate of 25-60 Hz. Blue light was used to excite the donor label for FRET excitation, generated by passing light from a white UHP-T2 LED head (Prizmatix, Southfield, MI) through an ET470/40x bandpass filter (Chroma, Bellows

Falls, VT) and T495lpdx dichroic (Chroma). The emission was passed through an ET500lp filter (Chroma) and split into two channels (donor/green and acceptor/red) by a T600lpdx dichroic (Chroma). An ET580/25x bandpass filter (Chroma) and T600lpdx dichroic (Chroma) were used for the excitation of mCherry. The magnitude of the temperature jumps is calibrated using the temperature-dependent quantum yield of mCherry.²²

Analysis of Thermodynamic Data Temperature melts of the proteins were collected using the average of the first 4 seconds of the equilibration (flat phase of the step function) after each jump. Thermodynamic data is plotted as the ratio of the donor (D) and acceptor (A) intensities (D/A) vs temperature. The resulting melting curves are fit to an apparent two-state equilibrium model:

$$S(T) = \{[S_D + m_D(T - 273.15)] + [S_N + m_N(T - 273.15)]e^{\frac{\Delta G}{RT}}\} / (1 + e^{-\Delta G/RT}) \quad (1)$$

where S_N and S_D are the signal contributions from the native (N) and denatured (D) populations at $T=273.15$ K (0 °C), m_D and m_N are the slope of the native and denatured state baseline and ΔG is the free energy of folding. We approximate the free energy of folding, $\Delta G \approx \Delta G_I(T-T_m)$ as a linear function of temperature.²²

Analysis of Kinetic Data To generate the kinetic data, the D/A is plotted against time. The kinetic data was fit to a double exponential:²²

$$S(t) = S_0 + A_1 e^{(t/\tau_{laser})} + A_2 e^{(t/\tau_{obs})^\beta} \quad (2)$$

where the first exponential accounts for the instrument response and relaxation of AcGFP,¹¹ and the second exponential accounts for the sample kinetics. S_0 is an offset, A_i are the amplitudes of the exponential decays, τ is the relaxation lifetime, and β is the stretched exponential factor. $\beta = 1$ for 2-state folders but may differ from one if there is multistate folding or in an inhomogeneous environment. β was held fixed at 1 for both the PGK and VlsE experiments presented here.

Supplementary Material

Supplementary material includes plots of the complete set of *in vitro* equilibrium temperature denaturation measurements, representative melt curves collected in living U-2 OS cells, and complete tables of thermodynamic and kinetic parameters obtained *in vitro* and in living U-2 OS cells.

Acknowledgements

This work was supported by the National Institutes of Health grant R01GM093318 (*in vitro* work) and National Science Foundation (NSF) grant NSF MCB 1803786 (in-cell work) to M.G. C.M.D. was supported in part by a postdoctoral fellowship provided by the PFC: Center for the Physics of Living Cells funded by NSF PHY 1430124.

Conflict of Interest

The authors declare no conflict of interest

References

1. Gierasch LM, Gershenson A (2009) Post-reductionist protein science, or putting Humpty Dumpty back together again. *Nat. Chem. Biol.* 5:774–777.
2. Zimmerman SB, Trach SO (1991) Estimation of macromolecule concentrations and excluded volume effects for the cytoplasm of *Escherichia coli*. *J. Mol. Biol.* 222:599–620.
3. Minton AP (1980) Excluded volume as a determinant of protein structure and stability. *Biophys. J.* 32:77–79.
4. Phillip Y, Sherman E, Haran G, Schreiber G (2009) Common crowding agents have only a small effect on protein-protein interactions. *Biophys. J.* 97:875–885.
5. Dhar A, Samiotakis A, Ebbinghaus S, Nienhaus L, Homouz D, Gruebele M, Cheung MS (2010) Structure, function, and folding of phosphoglycerate kinase are strongly perturbed by macromolecular crowding. *Proc. Natl. Acad. Sci.* 107:17586–17591.
6. Davis CM, Gruebele M (2018) Non-steric interactions predict the trend and steric interactions the offset of protein stability in cells. *ChemPhysChem* 19:2290–2294.
7. Zhou H-X, Rivas G, Minton AP (2008) Macromolecular crowding and confinement: biochemical, biophysical, and potential physiological consequences. *Annu. Rev. Biophys.* 37:375–97.
8. Acosta LC, Perez Goncalves GM, Pielak GJ, Gorenssek-Benitez AH (2017) Large cosolutes, small cosolutes, and dihydrofolate reductase activity. *Protein Sci.* 26:2417–2425.
9. Rivas G, Fernandez JA, Minton AP (2001) Direct observation of the enhancement of noncooperative protein self-assembly by macromolecular crowding: Indefinite linear self-association of bacterial cell division protein FtsZ. *Proc. Natl. Acad. Sci.* 98:3150–3155.
10. Danielsson J, Mu X, Lang L, Wang H, Binolfi A, Theillet F-X, Bekei B, Logan DT, Selenko P, Wennerström H, et al. (2015) Thermodynamics of protein destabilization in live cells. *Proc. Natl. Acad. Sci.* 112:12402–12407.
11. Guzman I, Gelman H, Tai J, Gruebele M (2014) The extracellular protein VlsE is destabilized inside cells. *J. Mol. Biol.* 426:11–20.
12. Tai J, Dave K, Hahn V, Guzman I, Gruebele M (2016) Subcellular modulation of protein VlsE stability and folding kinetics. *FEBS Lett.* 590:1409–1416.
13. Monteith WB, Pielak GJ (2014) Residue level quantification of protein stability in living cells. *Proc. Natl. Acad. Sci.* 111:11335–11340.
14. Sarkar M, Smith AE, Pielak GJ (2013) Impact of reconstituted cytosol on protein stability. *Proc. Natl. Acad. Sci.* 110:19342–19347.
15. Cohen RD, Pielak GJ (2016) Electrostatic contributions to protein quinary structure. *J. Am. Chem. Soc.* 138:13139–13142.
16. Mu X, Choi S, Lang L, Mowray D, Dokholyan N V., Danielsson J, Oliveberg M (2017) Physicochemical code for quinary protein interactions in *Escherichia coli*. *Proc. Natl. Acad. Sci.* 114:E4556–E4563.
17. Majumder S, Xue J, Demott CM, Reverdatto S, Burz DS, Shekhtman A (2015) Probing protein quinary interactions by in-cell nuclear magnetic resonance spectroscopy. *Biochemistry* 54:2727–2738.

18. Barbieri L, Luchinat E, Banci L (2015) Protein interaction patterns in different cellular environments are revealed by in-cell NMR. *Sci. Rep.* 5:14456.
19. Sarkar M, Li C, Pielak GJ (2013) Soft interactions and crowding. *Biophys. Rev.* 5:187–194.
20. Demott CM, Majumder S, Burz DS, Reverdatto S, Shekhtman A (2017) Ribosome Mediated Quinary Interactions Modulate In-Cell Protein Activities. *Biochemistry* 56:4117–4126.
21. Ebbinghaus S, Dhar A, McDonald JD, Gruebele M (2010) Protein folding stability and dynamics imaged in a living cell. *Nat. Methods* 7:319–323.
22. Dhar A, Girdhar K, Singh D, Gelman H, Ebbinghaus S, Gruebele M (2011) Protein stability and folding kinetics in the nucleus and endoplasmic reticulum of eucaryotic cells. *Biophys. J.* 101:421–430.
23. Benton LA, Smith AE, Young GB, Pielak GJ (2012) Unexpected Effects of Macromolecular Crowding on Protein Stability. *Biochemistry* 51:9773–9775.
24. Banani SF, Lee HO, Hyman AA, Rosen MK (2017) Biomolecular condensates: Organizers of cellular biochemistry. *Nat. Rev. Mol. Cell Biol.* 18:285–298.
25. Pozdnyakova I, Wittung-Stafshede P (2010) Non-linear effects of macromolecular crowding on enzymatic activity of multi-copper oxidase. *Biochim. Biophys. Acta - Proteins Proteomics* 1804:740–744.
26. Suthar MK, Doharey PK, Verma A, Saxena JK (2013) Behavior of Plasmodium falciparum purine nucleoside phosphorylase in macromolecular crowded environment. *Int. J. Biol. Macromol.* 62:657–662.
27. Rivas G, Ferrone F, Herzfeld J (2004) Life in a crowded world. *EMBO Rep.* 5:23–27.
28. Stadtmiller SS, Gorensek-Benitez AH, Guseman AJ, Pielak GJ (2017) Osmotic Shock Induced Protein Destabilization in Living Cells and Its Reversal by Glycine Betaine. *J. Mol. Biol.* 429:1155–1161.
29. Plaxco KW, Simons KT, Ruczinski I, Baker D (2000) Topology, Stability, Sequence, and Length: Defining the Determinants of Two-State Protein Folding Kinetics. *Biochemistry* 39:11177–11183.
30. Gelman H, Wirth AJ, Gruebele M (2016) ReAsH as a Quantitative Probe of In-Cell Protein Dynamics. *Biochemistry* 55:1968–1976.
31. Dhar A, Ebbinghaus S, Shen Z, Mishra T, Gruebele M (2010) The Diffusion Coefficient for PGK Folding in Eukaryotic Cells. *Biophys. J.* 99:L69–L71.
32. Xia Z, Das P, Shakhnovich EI, Zhou R (2012) Collapse of Unfolded Proteins in a Mixture of Denaturants. *J. Am. Chem. Soc.* 134:18266–18274.
33. Ganguly P, Shea J-E (2019) Distinct and Nonadditive Effects of Urea and Guanidinium Chloride on Peptide Solvation. *J. Phys. Chem. Lett.* 10:7406–7413.
34. Guin D, Gelman H, Wang Y, Gruebele M (2019) Heat shock-induced chaperoning by Hsp70 is enabled in-cell Sanchez-Ruiz JM, editor. *PLoS One* 14:e0222990.
35. Kisley L, Serrano KA, Guin D, Kong X, Gruebele M, Leckband DE (2017) Direct Imaging of Protein Stability and Folding Kinetics in Hydrogels. *ACS Appl. Mater. Interfaces* 9:21606–21617.
36. Humphrey W, Dalke A, Schulten K (1996) VMD: Visual molecular dynamics. *J. Molec.*

Graph. 14:33–38.

Figure Legends

Fig. 1. Schematic representation of PGK-FRET (A) and VlsE-FRET (B). Doubly labeled FRET complexes are labeled at the N-terminus with AcGFP1 and at the C-terminus with mCherry. Ribbon structures of VlsE (PDB ID: 1L8W), PGK (PDB ID: 1QPG), GFP (PDB ID: 1GFL), and mCherry (PDB ID: 2H5Q) were generated in VMD³⁶ and assembled in Adobe Photoshop CC.

Fig. 2. PGK (left) in 20 mM sodium phosphate buffer pH 7 and VlsE (right) in 10 mM sodium phosphate buffer pH 7. (A, B) Thermal stability at a constant lysis buffer concentration as a function of Ficoll concentration. (C, D) Thermal stability at a constant Ficoll concentration as a function of lysis buffer concentration. Melting temperatures (T_m) were extracted from a two-state model (Equation 1) fit of the thermal unfolding curves. Error bars shown reflect one standard deviation error in the fit of T_m . Each titration under a constant condition is fit to a straight line.

Fig. 3. Top: Change in thermal stability of PGK (left) and VlsE (right) in mixtures of Ficoll and lysis buffer relative to phosphate buffer-only (20 mM sodium phosphate for PGK, 10 mM for VlsE, both pH 7). Bottom: Same data, but relative to the stability of PGK and VlsE in-cell: ΔT_m is the difference in stability between the reported condition and the protein stability in living U-2 OS cells. The condition that best matches the cell, 150 mg/ml Ficoll and 60% lysis buffer, is outlined in black. Note: data was not collected for PGK at 0% lysis buffer and 150 mg/ml Ficoll.

Fig. 4. Representative relaxation kinetics of PGK (left) and VlsE (right) following a temperature jump to T_m obtained by FReI. *In vitro* experiments were conducted in sodium phosphate buffer (blue), sodium phosphate with 250 mg/ml Ficoll PM 70 (green), sodium phosphate with 60% Pierce IP lysis Buffer and 150 mg/ml Ficoll PM 70 (orange), and sodium phosphate buffer with 75% Pierce IP lysis Buffer (red). This is compared to relaxation kinetics measured in living U-2 OS cells (○). The signal from the two-color FRET experiments is reported as a donor/acceptor (D/A) ratio, normalized between 0 and 1. A double exponential fit (Equation 2) is overlaid on the data (---). The first exponential accounts for the instrument response and relaxation of AcGFP1. The second exponential is the sample kinetics.

Figure 1

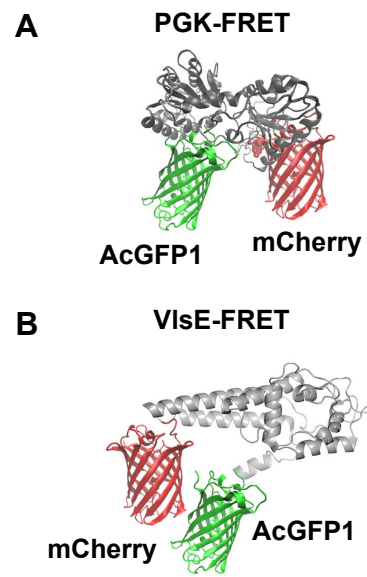


Figure 2

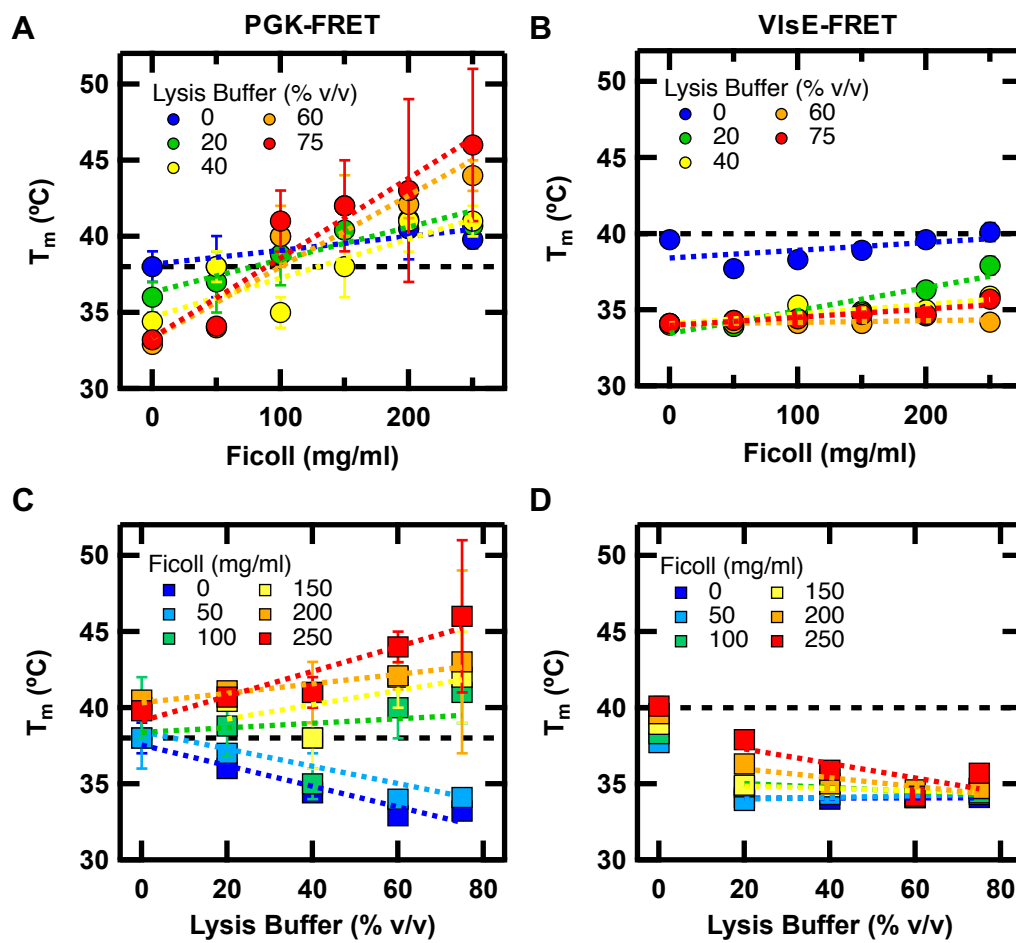


Figure 3

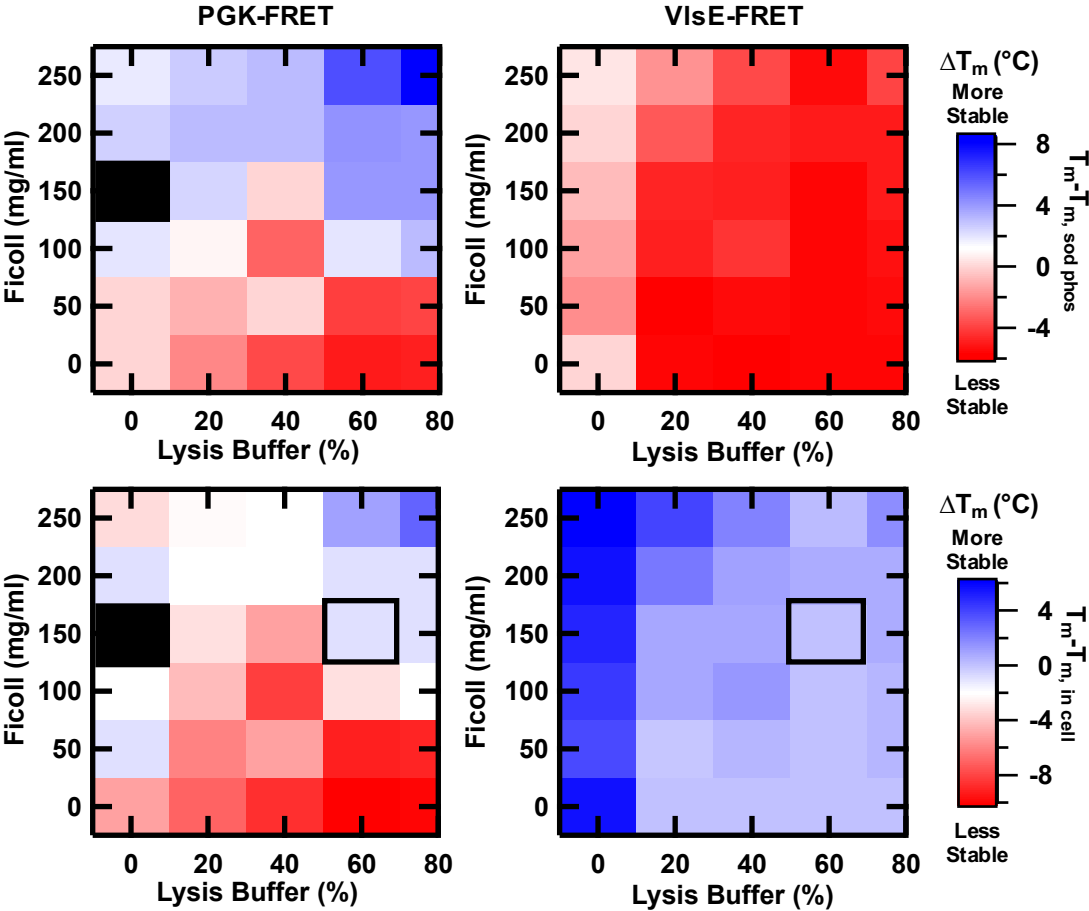


Figure 4

